CD93 negatively regulates astrogenesis in response to MMRN2 through the transcriptional repressor ZFP503 in the developing brain

Qingli Liang[a,b], Libo Su[a,b], Dongming Zhang[a,b], and Jianwei Jiao[a,b,c,d,1]

[a]State Key Laboratory of Stem Cell and Reproductive Biology, Institute of Zoology, Chinese Academy of Sciences, 100101 Beijing, China; [b]Medical School, University of Chinese Academy of Sciences, 100049 Beijing, China; [c]Co-Innovation Center of Neuroregeneration, Nantong University, 226001 Nantong, China; and [d]Innovation Academy for Stem Cell and Regeneration, 100101 Beijing, China

Edited by Jonathan Kipnis, University of Virginia, Charlottesville, VA, and accepted by Editorial Board Member Nancy Y. Ip March 12, 2020 (received for review December 30, 2019)

Astrogenesis is repressed in the early embryonic period and occurs in the late embryonic period. A variety of external and internal signals contribute to the sequential differentiation of neural stem cells. Here, we discovered that immune-related CD93 plays a critical negative role in the regulation of astrogenesis in the mouse cerebral cortex. We show that CD93 expression is detected in neural stem cells and neurons but not in astrocytes and declines as differentiation proceeds. *Cd93* knockout increases astrogenesis at the expense of neuron production during the late embryonic period. CD93 responds to the extracellular matrix protein Multimerin 2 (MMRN2) to trigger the repression of astrogenesis. Mechanistically, CD93 delivers signals to β-Catenin through a series of phosphorylation cascades, and then β-Catenin transduces these signals to the nucleus to activate *Zfp503* transcription. The transcriptional repressor ZFP503 inhibits the transcription of *glial fibrillary acidic protein* (*Gfap*) by binding to the *Gfap* promoter with the assistance of Grg5. Furthermore, *Cd93* knockout mice exhibit autism-like behaviors. Taken together, our results reveal that CD93 is a negative regulator of the onset of astrogenesis and provide insight into therapy for psychiatric disorders.

CD93 | astrogenesis | ZFP503 | repression | MMRN2

Neurogenesis precedes astrogenesis during brain development. Until the late embryonic stage, radial glial cells differentiate into astrocytes; meanwhile, some radial glial cells are still able to differentiate into neurons to complete neurogenesis (1–8). How can radial glial cells control the precise timing of neuronal or astrocyte differentiation? Astrogenesis is repressed during the neurogenic period and derepressed in the late embryonic stage. In the early embryonic stage, astrocytic gene promoters undergo DNA methylation and H3K9 methylation, which inhibit transcription (9, 10). bHLH transcription factors, such as Ngn1, sequester a combination of phosphorylated signal transducer and activator of transcription 3 (pSTAT3) and the cofactor complex Smad/CBP/p300 (11). Transcriptional repressors such as N-CoR inhibit astrocytic gene expression (12).

After derepression of astrogenesis, several classical signaling pathways, such as the JAK-STAT3, Notch, and BMP pathways, promote astrocytic fate determination in radial glial cells (13–16). Beyond these pathways, there are also some other external and internal signals involved in this process. Here, we focus on extracellular matrix (ECM) proteins and their receptors. Many studies have reported that ECM proteins participate in the differentiation of neural stem cells (17–21). As the receptors of ECM proteins, integrins deliver signals from the niche and trigger some signaling pathways to influence the fate determination of stem cells, including neural progenitors (21–23).

CD93, also named AA4 and C1qRp in humans, is a single transmembrane glycoprotein expressed on the surface of various cell types (24, 25). Previous works have shown that CD93 plays an important role in signal transduction. Many studies have identified its functions in adhesion, angiogenesis, and hematopoietic stem cell homing (25–27), and other studies have revealed its functions in innate immunity and inflammation (25, 26, 28, 29). Several of these studies have demonstrated CD93's role in regulating central nervous system inflammation (28, 29). However, whether CD93 functions in the fate determination of radial glial cells in the developing cortex has yet to be elucidated. Although CD93 was originally cloned due to its possible ability to regulate phagocytosis induced by C1q (30), a later study demonstrated that C1q can enhance the phagocytosis of macrophages from CD93-null mice (31), and human C1qRp has also been reported to not be the receptor for C1q (27). Therefore, C1q is not the ligand for CD93 (25). Recently, studies have proven that CD93 interacts with the ECM protein Multimerin 2 (MMRN2) to deliver integrin-dependent signals (32–34). We wondered whether these external signals influence the fate determination of radial glial cells.

Here, we demonstrate that CD93 plays a negative role in regulating astrogenesis. We have identified that CD93 is expressed in neural stem cells and represses the onset of astrogenesis in response to the ECM-signaling molecule MMRN2. *Cd93* knockout increases astrogenesis at the expense of neuron production, and abnormal differentiation contributes to autism-like behaviors.

Significance

Astrogenesis occurs during sequential differentiation of neural stem cells. This is because astrocyte production is repressed in the early embryonic stage, but the reasons for this repression need to be comprehensively understood. External and internal signals must contribute to this phenomenon. The signal trigger requires two factors: the ligand and receptor. Which ligand in the niche is involved? Which receptor in the membrane of neural stem cells is involved? Here, we focus on a receptor named CD93, which is known for its immune functions. We reveal its function in the differentiation of neural stem cells independent of immunity. CD93 responds to MMRN2 to control the proper timing of astrogenesis. In conclusion, our study identifies a negative regulator in astrogenesis.

Author contributions: Q.L. and J.J. designed research; J.J. supervised the research; Q.L. and D.Z. performed research; L.S. contributed new reagents/analytic tools; Q.L. analyzed data; Q.L. and J.J. wrote the paper; and L.S. provided some suggestions for the research.

The authors declare no competing interest.

This article is a PNAS Direct Submission. J.K. is a guest editor invited by the Editorial Board.

Data deposition: Transcriptome sequencing data reported in this article have been deposited in the Gene Expression Omnibus database (accession no. GSE134642).

[1]To whom correspondence may be addressed. Email: jwjiao@ioz.ac.cn.

This article contains supporting information online at https://www.pnas.org/lookup/suppl/doi:10.1073/pnas.1922713117/-/DCSupplemental.

First published April 14, 2020.

CD93 delivers signal to the nucleus to regulate *Zfp503* transcription through a series of phosphorylation cascades, and ZFP503 represses the transcription of *Gfap*. Taken together, our results identify a critical regulator of the timing of astrogenesis.

Results

CD93 Expression Pattern in the Developing Cerebral Cortex. We first examined the CD93 expression pattern in the developing cerebral cortex. Immunostaining showed that CD93 was widely expressed across embryonic day (E) 13 cortex, especially in the ventricular zone (VZ) and subventricular zone (SVZ) (Fig. 1*A*). At E16, CD93 was expressed not only in the VZ/SVZ but also in the cortical plate, where neurons were located (Fig. 1*A*). We further confirmed that CD93 was obviously colocalized with NESTIN, which labels neural stem cells, in the VZ/SVZ at both E13 and E16 (Fig. 1*A*). In vitro immunostaining also clearly showed that CD93 was abundantly expressed in NESTIN-labeled neural stem cells and MAP2-labeled neurons (Fig. 1 *B* and *C*), while there was low or no expression in most astrocytes and oligodendrocytes (Fig. 1 *D* and *E*). As differentiation proceeded in vitro, we examined whether *Cd93* messenger RNA (mRNA) levels declined (Fig. 1*F*). We further detected that *Cd93* mRNA levels were decreased in radial glial cells in the developing cortex from E14 to postnatal day 0 (P0) (Fig. 1*G*). These results showed that CD93 probably plays opposite roles in the production of neurons and astrocytes.

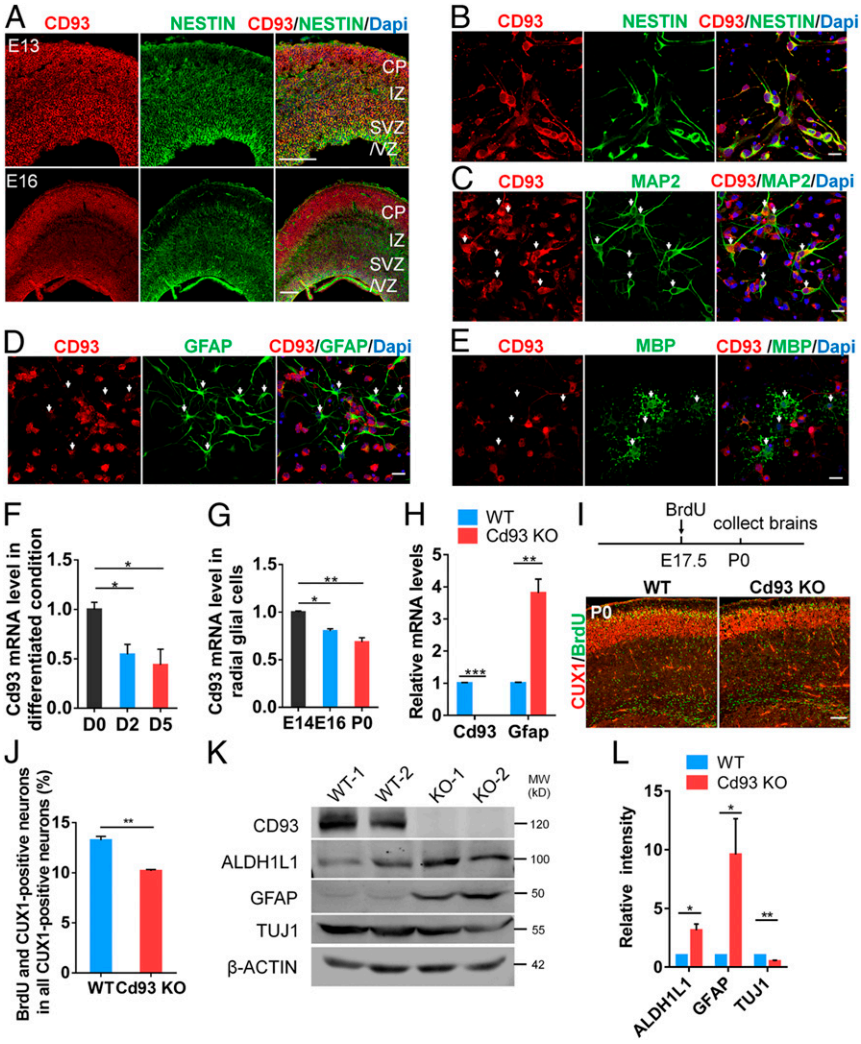

Fig. 1. The CD93 expression pattern and its role in regulating cell-fate determination in the developing cerebral cortex. (*A*) Immunostaining for CD93 and NESTIN in the E13 and E16 cerebral cortex. (Scale bars, 100 μm.) (*B–E*) Immunostaining for CD93 in different cell types in vitro. E16 neural stem cells were isolated and cultured in proliferation medium for 1 d before being immunostained for NESTIN (*B*), cultured in differentiation medium for 4 d before being immunostained for MAP2 and GFAP (*C* and *D*), or cultured in differentiation medium for 6 d before being immunostained for MBP (*E*). The arrows in *C* show that CD93 was expressed in MAP2-labeled neurons. The arrows in *D* and *E* show that CD93 was not expressed in GFAP-labeled astrocytes or MBP-labeled oligodendrocytes. (Scale bars, 20 μm.) (*F*) *Cd93* mRNA levels were detected during differentiation in vitro. E13 neural stem cells were isolated, cultured in differentiation medium, and collected on day 0, day 2, or day 5. $n = 3$ independent experiments. (*G*) *Cd93* mRNA levels were detected in radial glial cells at E14, E16, or P0. $n = 3$ mice per age. (*H*) *Cd93* and *Gfap* mRNA levels were detected in the E18 cerebral cortex of *Cd93* knockout and wild-type mice. $n = 5$ wild-type mice and 5 *Cd93* knockout mice. (*I*) A BrdU birthdating experiment was used to detect neuron production in the late embryonic stage. BrdU was injected into pregnant mice at E17.5, and the brains were collected at P0 and immunostained for CUX1 and BrdU. (Scale bar, 100 μm.) (*J*) Quantification of the percentage of BrdU- and CUX1-positive cells in *I*. $n = 3$ wild-type mice and 3 *Cd93* knockout mice. (*K*) *Cd93* knockout changed the protein levels of CD93, ALDH1L1, GFAP, and TUJ1 in the E18 cerebral cortex. (*L*) Quantification of the protein levels in *K*. $n = 3$ wild-type mice and 3 *Cd93* knockout mice. Statistical analysis was performed using Student's *t* test for comparisons of two groups and one-way ANOVA for comparisons of more than two groups. The error bars show mean ± SEM; $*P < 0.05$; $**P < 0.01$; $***P < 0.001$.

***Cd93* Knockout Promotes Astrogenesis and Inhibits Neurogenesis in the Late Embryonic Stage.** To investigate our hypothesis, we generated *Cd93* knockout mice with the CRISPR-Cas9 system (*SI Appendix*, Fig. S1 *A–C*). Quantitative real-time PCR and Western blotting validated the knockout efficiency at the mRNA and protein levels, respectively (Fig. 1*H* and *SI Appendix*, Fig. S1*D*). Immunostaining also confirmed that there was no expression of CD93 in the knockout brain at E13 (*SI Appendix*, Fig. S1*E*). To detect whether CD93 plays a role in astrocytic differentiation, we performed the following experiments. Quantitative real-time PCR showed that the mRNA level of the astrocyte marker *Gfap* increased in the *Cd93* knockout cortex at E18 (Fig. 1*H*). Western blotting further showed that *Cd93* knockout increased the protein levels of the astrocyte markers GFAP and aldehyde dehydrogenase 1 family member L1 (ALDH1L1) in the E18 cortex (Fig. 1 *K* and *L*). On the other hand, we wondered whether CD93 affects neurogenesis in this stage. We first performed a BrdU birthdating experiment and found that *Cd93* knockout decreased the production of neurons in the late embryonic stage (Fig. 1 *I* and *J*). Western blotting further confirmed that *Cd93* knockout decreased the protein level of the neuronal marker class III beta-tubulin (TUJ1) in the E18 cortex (Fig. 1 *K* and *L*). These results showed that *Cd93* knockout disrupted the balance between neurogenesis and astrogenesis in the late embryonic stage. Accordingly, we hypothesize that CD93 may be a barrier to astrogenesis onset.

***Cd93* Knockout Derepresses and Enhances Astrogenesis.** To investigate the role of CD93 in astrogenesis onset, we performed a series of immunostaining assays to detect changes in astrogenesis. The increase in the number of brain lipid-binding protein (BLBP)-positive astrocyte progenitors observed at E16 and E18 showed that *Cd93* knockout promoted the astrocytic specification of radial glial cells (Fig. 2 *A–D*). Beginning at E18, the number of GFAP-positive astrocytes in *Cd93* knockout mice was higher than that in wild-type mice, and we further detected an increase at P2 (Fig. 2 *E–H*). Beginning at E16, *Cd93* knockout resulted in the production of more S100β-positive astrocytes, and we sequentially detected increases at E18, P2, and P5 (Fig. 2 *I–P*). Moreover, astrocyte morphology was more abundant in *Cd93* knockout mice than in wild-type mice (Fig. 2*M*). We detected a dose-dependent increase in the production of S100β-positive astrocytes in *Cd93* heterozygous and knockout mice (*SI Appendix*, Fig. S2 *A* and *B*). These results indicate that CD93 plays an important role in controlling the precise timing of astrogenesis onset and that *Cd93* knockout derepresses and enhances astrogenesis.

***Cd93* Knockout Results in Persistent Increased Astrocyte Production and Decreased Neuron Production in the Developing Cortex.** We performed long-term detection of astrocyte production in vivo. At P7, the number of GFAP- and S100β-positive astrocytes in *Cd93* knockout mice was obviously higher than that in wild-type mice (Fig. 3 *A–D*). The number of GS-positive astrocytes increased in *Cd93* knockout mice at P12 (Fig. 3 *E* and *F*). At P14, we detected continued elevation of GFAP- and ACSBG1-positive astrocyte production (Fig. 3 *G–J*). These results indicated that there is persistent increased production of astrocyte in the cerebral cortex of *Cd93* knockout mice.

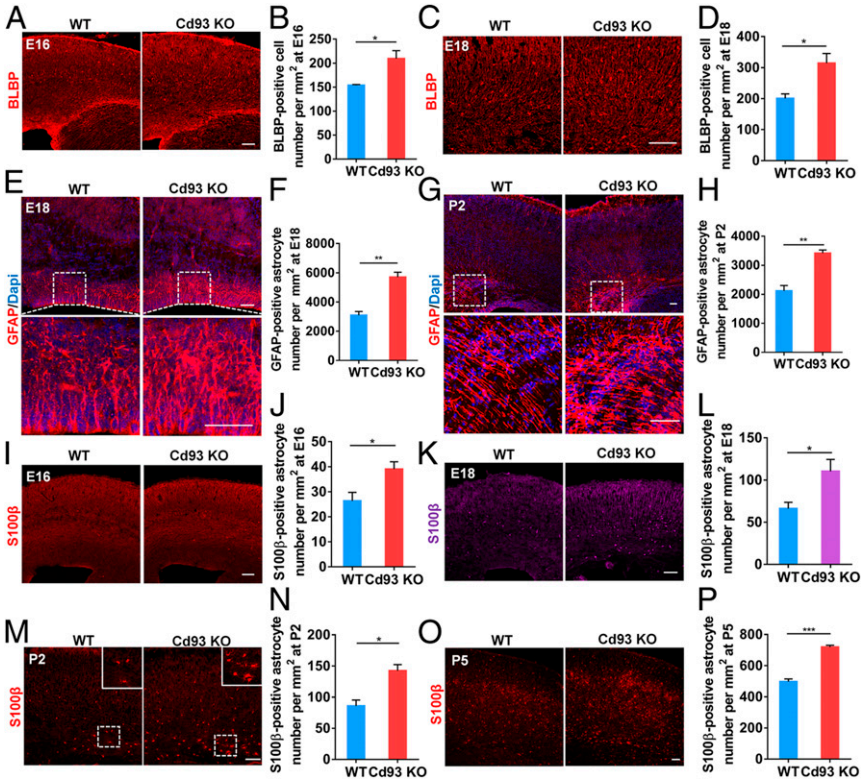

Fig. 2. Astrogenesis is enhanced in *Cd93* knockout mice. (*A–D*) The number of BLBP-positive astrocyte progenitors in the cerebral cortex of wild-type and *Cd93* knockout mice at E16 (*A* and *B*) and E18 (*C* and *D*) was determined. $n = 3$ wild-type mice and 4 *Cd93* knockout mice at E16; $n = 3$ wild-type mice and 3 *Cd93* knockout mice at E18. (Scale bars, 100 μm.) (*E–H*) The number of GFAP-positive astrocytes per square millimeter in wild-type and *Cd93* knockout mice at E18 (*E* and *F*) and P2 (*G* and *H*) was determined. $n = 3$ wild-type mice and 4 *Cd93* knockout mice at E18; $n = 3$ wild-type mice and 3 *Cd93* knockout mice for P2. (Scale bars, 50 μm.) (*I–P*) The number of S100β-positive astrocytes in the cerebral cortex of wild-type and *Cd93* knockout mice at E16 (*I* and *J*), E18 (*K* and *L*), P2 (*M* and *N*), and P5 (*O* and *P*) was determined. $n = 3$ wild-type mice and 4 *Cd93* knockout mice at E16; $n = 3$ wild-type mice and 3 *Cd93* knockout mice at E18, P2, and P5. (Scale bars, 100 μm.) Statistical analysis was performed using Student's *t* test. The error bars show mean ± SEM; $^{*}P < 0.05$; $^{**}P < 0.01$; $^{***}P < 0.001$.

To determine whether the overall development of cortex is affected in *Cd93* knockout mice, we investigated neuronal development at a number of postnatal time points. Immunostaining showed that the NeuN-positive neuron number was decreased at P0, P2, and P12 in *Cd93* knockout mice (*SI Appendix*, Fig. S3 *A–F*). Then we analyzed the cortical layers at P2. Although there was no difference in the early born TBR1- and CTIP2-positive neurons, the production of SATB2-positive neurons decreased in *Cd93* knockout mice (*SI Appendix*, Fig. S3 *G* and *H*). We did not find difference in the area of the cerebral cortex at P12, and we speculated that that was caused by the switch between astrogenesis and neurogenesis in *Cd93* knockout mice (*SI Appendix*, Fig. S3 *I* and *J*).

No Peripheral Inflammation Was Detected in *Cd93* Knockout Mice. As CD93 may play roles in peripheral immunity, we performed a series of experiments to determine whether there is peripheral inflammation in *Cd93* knockout mice. We first measured the protein levels of the proinflammatory cytokines IL-6 and IL-1β in the brain and did not find any increase in *Cd93* knockout mice (*SI Appendix*, Fig. S4 *A* and *B*). We also did not find an increase in the iNOS expression level (*SI Appendix*, Fig. S4 *A* and *B*). Enzyme-linked immunosorbent assay (ELISA) showed no increase of TNFα level in the blood of *Cd93* knockout mice (*SI Appendix*, Fig. S4*C*). Immunostaining showed that *Cd93* knockout did not activate microglia (*SI Appendix*, Fig. S4 *D* and *E*). Blood–brain barrier integrity in *Cd93* knockout mice seemed normal as was that of wild-type mice, as evaluated by Cad-A555 (*SI Appendix*, Fig. S4*F*). These results of our detection show that there is no inflammation in *Cd93* knockout mice and exclude the possibility of reactive gliosis.

***Cd93* Knockout Contributes to Autism-Like Behaviors in Mice.** As *Cd93* knockout disrupts the balance of astrogenesis and neurogenesis in the late embryonic stage, we wondered whether abnormal development triggers any behavioral defects in *Cd93* knockout mice. The open field test showed that *Cd93* knockout mice traveled a longer distance than wild-type mice, and the result indicated that *Cd93* knockout mice showed hyperactivity (Fig. 4 *A* and *B* and *SI*

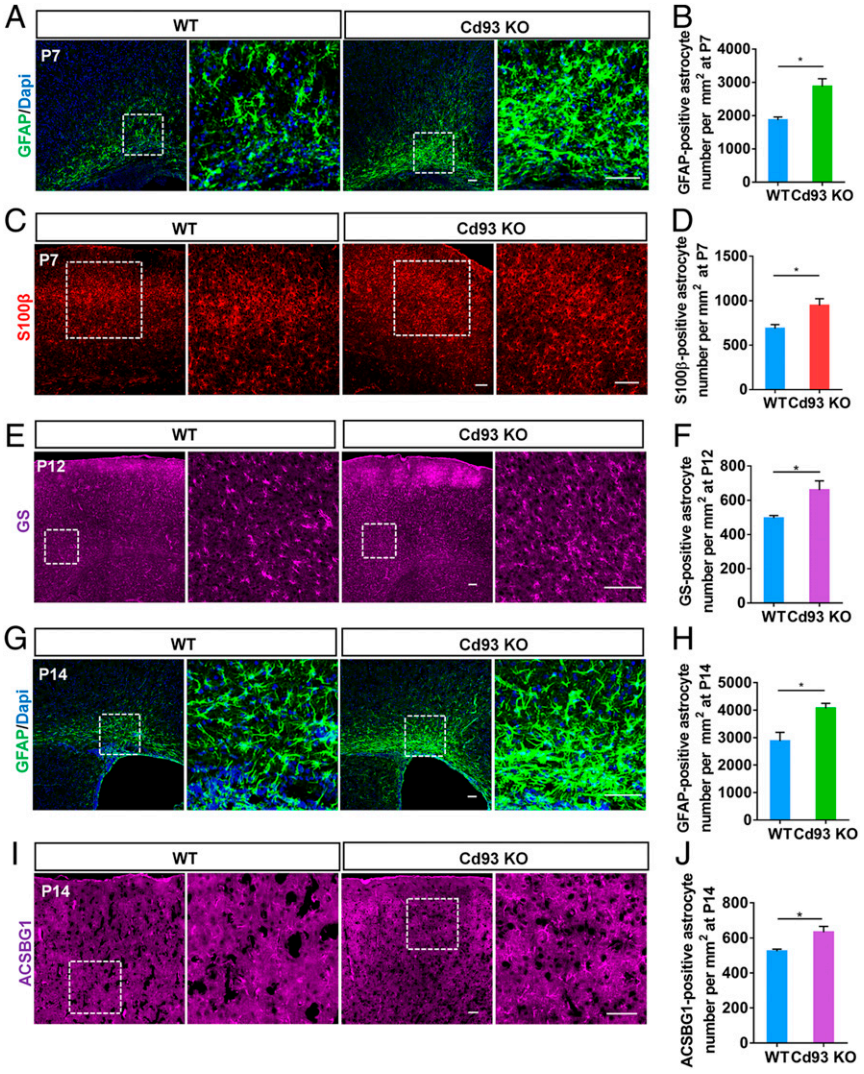

Fig. 3. Persistent increase in astrocyte production in the *Cd93* knockout cortex. (*A*, *B*, *G*, and *H*) The number of GFAP-positive astrocytes per square millimeter at P7 and P14 was determined. $n = 3$ wild-type mice and 4 *Cd93* knockout mice for P7; $n = 3$ wild-type mice and 3 *Cd93* knockout mice for P14. (Scale bars, 50 μm.) (*C* and *D*) The number of S100β-positive astrocytes at P7 was determined. $n = 3$ wild-type mice and 3 *Cd93* knockout mice. (Scale bars, 100 μm.) (*E* and *F*) The number of GS-positive astrocytes in the cerebral cortex at P12 was determined. $n = 3$ wild-type mice and 3 *Cd93* knockout mice. (Scale bars, 100 μm.) (*I* and *J*) The number of ACSBG1-positive astrocytes in the cerebral cortex at P14 was determined. $n = 3$ wild-type mice and 3 *Cd93* knockout mice. (Scale bars, 50 μm.) Statistical analysis was performed using Student's *t* test. The error bars show mean ± SEM; $^*P < 0.05$.

Appendix, Fig. S5*A*). The elevated plus-maze test showed that *Cd93* knockout mice spent more time in the closed arms and less time in the open arms than wild-type mice, and the results indicate that *Cd93* knockout mice showed anxiety-like behavior and exploration deficiency (Fig. 4 *C* and *D* and *SI Appendix*, Fig. S5*B*).

To test whether *Cd93* knockout mice exhibit deficiencies in social interaction, we performed a three-chamber social interaction test. During the second phase, the wild-type mice showed great interest in the stranger 1 mouse, while *Cd93* knockout mice did not show significant interest in the stranger 1 mouse (Fig. 4*E* and *SI Appendix*, Fig. S5*C*). When the stranger 2 mouse was put into the empty cage, the wild-type mice spent more time interacting with the stranger 2 mouse than with the familiar stranger 1 mouse. However, *Cd93* knockout mice did not show more interest in the stranger 2 mouse (Fig. 4*F* and *SI Appendix*, Fig. S5*D*). These results indicate that *Cd93* knockout disrupted social interaction abilities.

According to the phenotype of *Cd93* knockout mice, we speculated that *Cd93* knockout might cause autism-like behavior. To test this hypothesis, we performed an ultrasonic vocalization (USV) test on pups at P10. When isolated from their mothers and littermates, *Cd93* knockout pups emitted shorter call durations and produced fewer calls than wild-type pups (Fig. 4 *G*–*I*). These results are consistent with autism behavior, which generally arises from childhood.

To further test this hypothesis, we monitored the repetitive behaviors of adult mice. We observed that the time spent self-grooming and times of jumping increased, although there was no significant difference (*SI Appendix*, Fig. S5 *E* and *F*). The marble-burying test showed that *Cd93* knockout mice buried more marbles than wild-type mice, indicating that *Cd93* knockout mice dug more frequently (Fig. 4*J* and *SI Appendix*, Fig. S5*G*).

Taken together, these results demonstrate that *Cd93* knockout mice exhibit defects in behavior. Hyperactivity, anxiety, defects in exploratory activity and sociability, defects in the USV experiment and repetitive behaviors indicate that *Cd93* knockout mice are prone to autism-like behaviors.

CD93 Regulates the Fate Determination of Radial Glial Cells in Response to the ECM Protein MMRN2. What kind of external signal does CD93 receive to trigger the above changes? Previous works have reported that ECM protein MMRN2 may be the ligand of CD93 (32, 34). We performed a co-immunoprecipitation (Co-IP) experiment to test the interaction between CD93 and MMRN2. The results showed that Flag-tagged CD93 clearly pulled down HA-tagged MMRN2 and that HA-tagged MMRN2 similarly pulled down Flag-tagged CD93 (Fig. 5 *A* and *B*). We further tested the interaction in vivo (*SI Appendix*, Fig. S6*A*). To visualize their interaction, we performed immunostaining and found that CD93 colocalized with MMRN2 in the cell membrane of N2a cells (Fig. 5*C*). To validate the effect of MMRN2, we first performed in utero electroporation. Immunostaining showed that the overexpression of MMRN2 inhibited the production of GFAP-positive astrocytes (Fig. 5 *D* and *E*). When we added

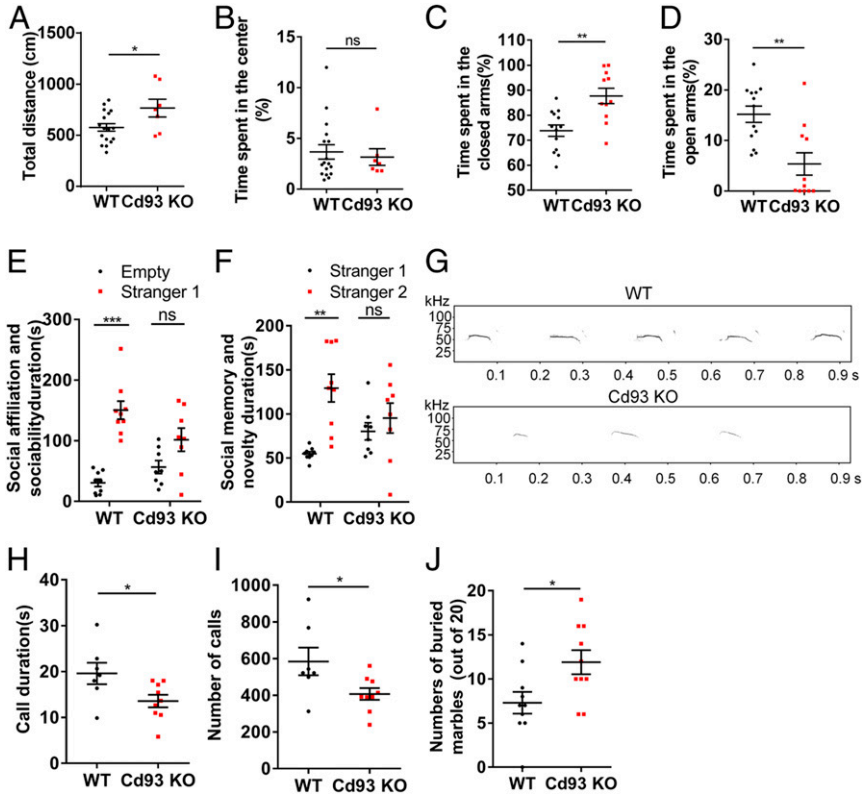

Fig. 4. *Cd93* knockout mice show autism-like behaviors. (*A* and *B*) The total distance traveled (*A*) and the time spent in the center (*B*) in the open field test. $n = 17$ wild-type mice and 7 *Cd93* knockout mice. (*C* and *D*) The time spent in closed arms (*C*) and open arms (*D*) in the elevated plus-maze test. $n = 13$ wild-type mice and 11 *Cd93* knockout mice. (*E* and *F*) Social affiliation and sociability duration (*E*) in the sociability session and social memory and novelty duration (*F*) in the social novelty preference session in the three-chamber social interaction test. $n = 9$ wild-type mice and 8 *Cd93* knockout mice. (*G*–*I*) Representative images (*G*) and the call duration (*H*) and number of calls (*I*) for USVs in P10 pups. $n = 7$ wild-type mice and 9 *Cd93* knockout mice. (*J*) In the marble-burying test, the *Cd93* knockout mice buried a greater number of marbles. $n = 10$ wild-type mice and 10 *Cd93* knockout mice. Statistical analysis was performed using Student's *t* test for comparisons of two groups and two-way ANOVA for social interaction test. The error bars show mean ± SEM; ns, $P > 0.05$; $^{*}P < 0.05$; $^{**}P < 0.01$; $^{***}P < 0.001$.

MMRN2 to the medium, the number of GFAP-positive astrocytes decreased, and the number of TUJ1-positive neurons increased (Fig. 5 *F* and *G*). Furthermore, CD93 overexpression further promoted this effect (Fig. 5 *F* and *G*). We further validated the effect at the protein level in vitro (*SI Appendix*, Fig. S6 *B* and *C*). To further elucidate that the function of MMRN2 is dependent on the CD93 receptor, we isolated neural stem cells from the cortex of wild-type and *Cd93* knockout mice and cultured the cells in vitro. We found that *Cd93* knockout increased the proportion of GFAP-positive astrocytes and reduced the proportion of MAP2-positive neurons in the group not treated with MMRN2 (Fig. 5 *H* and *I*). When we added MMRN2, the proportion of GFAP-positive astrocytes was reduced and the proportion of MAP2-positive neurons increased in the wild-type group (Fig. 5 *H* and *I*). However, when *Cd93* was knocked out, the effect of MMRN2 was abolished (Fig. 5 *H* and *I*). To detect which cell type in the cerebral cortex secretes MMRN2, we performed an ELISA experiment. The results showed that MMRN2 was detected in the medium of E15 neural stem cells, which implied that it might be secreted in an autocrine manner (*SI Appendix*, Fig. S6*D*). These results indicated that CD93 responds to MMRN2 signaling to regulate the differentiation of radial glial cells.

CD93 Suppresses Astrogenesis through the Transcriptional Repressor ZFP503. To explore the internal mechanism by which CD93 suppresses the onset of astrogenesis, we performed RNA sequencing (RNA-seq) analysis at E16. Our results showed that *Cd93* knockout changed the gene expression profile in the cerebral cortex (Fig. 6*A*). Based on gene ontology analysis, we found that *Cd93* knockout influenced glial cell development and neurogenesis (Fig. 6 *B* and *C*). Moreover, a number of transcription factors related to radial glial cell differentiation were down-regulated (Fig. 6*D*). Among them, we noticed that ZFP503, a transcriptional repressor, was greatly reduced (Fig. 6 *D* and *E*). We further confirmed that *Cd93* knockout reduced *Zfp503* mRNA levels in radial glial cells at E16 and protein levels in the cortex at E18 (Fig. 6 *F*–*H*).

What is the role of ZFP503 in astrogenesis? We speculated that ZFP503 regulates astrogenesis by suppressing *Gfap* transcription. Immunostaining showed that ZFP503 was expressed in NESTIN-labeled neural stem cells, MAP2-labeled neurons, and GFAP-labeled astrocytes (*SI Appendix*, Fig. S7 *A*–*C*). To investigate our hypothesis, we designed two short hairpin RNAs and validated the knockdown efficiency (*SI Appendix*, Fig. S7 *D* and *E*). Immunostaining showed that the knockdown of ZFP503 increased the proportion of astrocytes and reduced the proportion

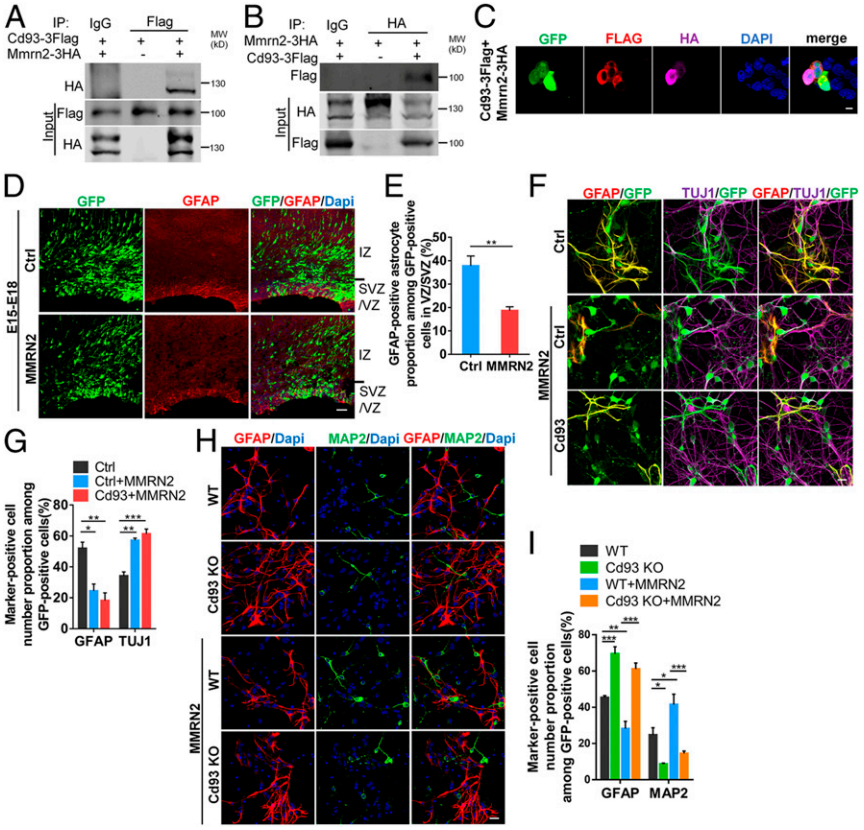

Fig. 5. The external signal ligand MMRN2 triggers regulation. (*A* and *B*) A Co-IP experiment was performed to detected the interaction between CD93 and MMRN2 in 293FT cells. (*C*) Immunostaining for FLAG and HA was performed to evaluate the colocalization of CD93 and MMRN2 in N2a cells. (Scale bar, 10um.) (*D*) Control and MMRN2 overexpression plasmids were electroporated into E15 brains, and the brains were collected 3 d later at E18. Immunostaining for GFAP was performed. (Scale bar, 50 μm.) (*E*) Quantification of the percentage of GFAP-positive astrocytes among GFP-positive cells in the VZ/SVZ. $n = 3$ mice for control (Ctrl) and 4 mice for MMRN2. (*F*) E16 neural stem cells were isolated, infected with the indicated lentivirus, and cultured in differentiation medium for 5 d. MMRN2 was added to the differentiation medium at a concentration of 100 ng/mL. Immunostaining for GFAP and TUJ1 was performed. (Scale bar, 20 μm.) (*G*) The proportion of GFAP-positive astrocytes and TUJ1-positive neurons among GFP-positive cells was quantified. $n = 3$ independent experiments. (*H*) E16 neural stem cells were isolated and cultured in differentiation medium with or without 100 ng/mL MMRN2 for 5 d before being immunostained for GFAP and MAP2. The embryos of wild-type and *Cd93* knockout were from the same pregnant heterozygous mice. (Scale bar, 20 μm.) (*I*) The percentage of GFAP- or MAP2-positive cells among all cells was quantified. $n = 3$ independent experiments. Statistical analysis was performed using one-way ANOVA or two-way ANOVA. The error bars show mean ± SEM; $^*P < 0.05$; $^{**}P < 0.01$; $^{***}P < 0.001$.

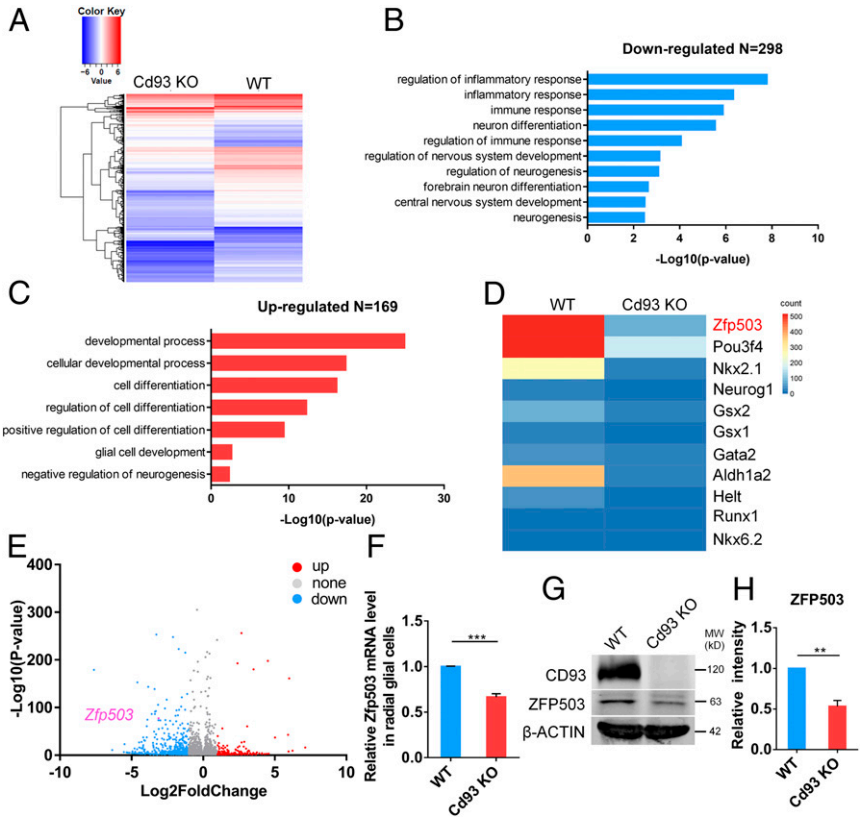

Fig. 6. RNA-seq analysis of the E16 cerebral cortex. (*A*) Heat map of RNA-seq data from the E16 cerebral cortex of wild-type and *Cd93* knockout brain. (*B* and *C*) Gene ontology analysis of down-regulated and up-regulated genes associated with biological functions related to immunity and differentiation in cerebral cortex. (*D*) Heat map of genes related to differentiation of radial glial cells in wild-type and *Cd93* knockout brains. (*E*) Volcano plots illustrating the down-regulated (blue) and up-regulated (red) genes in the *Cd93* knockout cerebral cortex compared with the wild-type cortex. *Zfp503* is labeled as a differentially expressed gene. (*F*) The *Zfp503* mRNA levels were reduced in E16 radial glial cells in the *Cd93* knockout cerebral cortex. $n = 4$ wild-type mice and 4 *Cd93* knockout mice. (*G*) ZFP503 protein levels were reduced at E18 in the *Cd93* knockout cerebral cortex. (*H*) Quantification of the protein level in *G*. $n = 3$ wild-type mice and 3 *Cd93* knockout mice. Statistical analysis was performed using Student's *t* test. The error bars show mean ± SEM; $^{**}P < 0.01$; $^{***}P < 0.001$.

of neurons (Fig. 7 *A* and *C*). At the same time, the overexpression of ZFP503 suppressed differentiation toward astrocytes and promoted differentiation toward neurons (Fig. 7 *B* and *D*).

To directly demonstrate the transcriptional repression of ZFP503, we cloned the human *Gfap* promoter into the psiCheck 2 vector and performed a luciferase assay. The results showed that ZFP503 repressed basal luciferase activity (Fig. 7*E*). Previous studies (35–37) have reported that ZFP503 does not bind to DNA sequences. How can it then repress the transcription of *Gfap*? Previous studies have reported that ZFP503 performs its function with the assistance of Grg5 (35). We confirmed that ZFP503 interacts with Grg5 through Co-IP experiments (Fig. 7 *F* and *G*). A chromatin immunoprecipitation (Ch-IP) assay demonstrated that Grg5 binds to the *Gfap* promoter 0.5, 1.5, and 2 kb upstream of the transcriptional start site (Fig. 7*H*). These results demonstrated that ZFP503 represses *Gfap* transcription through an interaction with the DNA-binding corepressor Grg5. Taken together, these results indicate that CD93 regulates astrogenesis through ZFP503.

β-Catenin Transduces the Signal from CD93 to ZFP503 through a Phosphorylation Cascade. How is the external signal delivered to the nucleus to regulate *Zfp503* transcription? We hypothesized that a protein in the cytoplasm is activated to transduce the signal into the nucleus. A previous study reported that β-Catenin binds to the promoter of *Zfp703*, which belongs to the same subfamily as *Zfp503*, and regulates *Zfp703* transcription (38–40). In mice, there is 54% identity between the *Zfp503* and *Zfp703* sequences (38, 40). To validate whether β-Catenin also activates *Zfp503* transcription, we performed a Ch-IP assay. The results showed that β-Catenin binds to the *Zfp503* promoter 0.5 kb upstream of the transcriptional start site (Fig. 7*I*). Immunostaining showed that the overexpression of β-Catenin inhibited differentiation toward astrocytes and promoted differentiation toward neurons (*SI Appendix*, Fig. S8 *A* and *B*). The knockdown of β-Catenin promoted differentiation toward astrocytes and inhibited differentiation toward neurons (*SI Appendix*, Fig. S8 *C* and *D*). Furthermore, treatment with the WNT agonist CHIR99021 rescued the phenotype of *Cd93* knockout mice (*SI Appendix*, Fig. S8 *E* and *F*).

To determine the signaling pathway linking CD93 to β-Catenin, we examined previous studies. We found that the interaction between CD93 and MMRN2 is essential for the phosphorylation of focal adhesion kinase (FAK) at Tyr397 by integrin α5β1 (34, 41). Studies have shown that β1 integrin is abundantly expressed in neural stem cells and participates in signal transduction from the niche (21, 23, 42). Activated FAK phosphorylates AKT at Ser473, and AKT phosphorylates GSK3β at Ser9. β-Catenin is then free to translocate into the nucleus (43–45). To validate this signaling pathway, we measured protein levels. The results showed that *Cd93* knockout reduced the phosphorylation of FAK and AKT and that the phosphorylation of GSK3β at Ser9 was reduced while the phosphorylation of GSK3β at Y216 increased (Fig. 7 *J* and *K*). Accordingly, β-Catenin was phosphorylated and degraded, and active β-Catenin was reduced (Fig. 7 *J* and *K*). These results demonstrate that CD93 delivers signals to β-Catenin through a phosphorylation

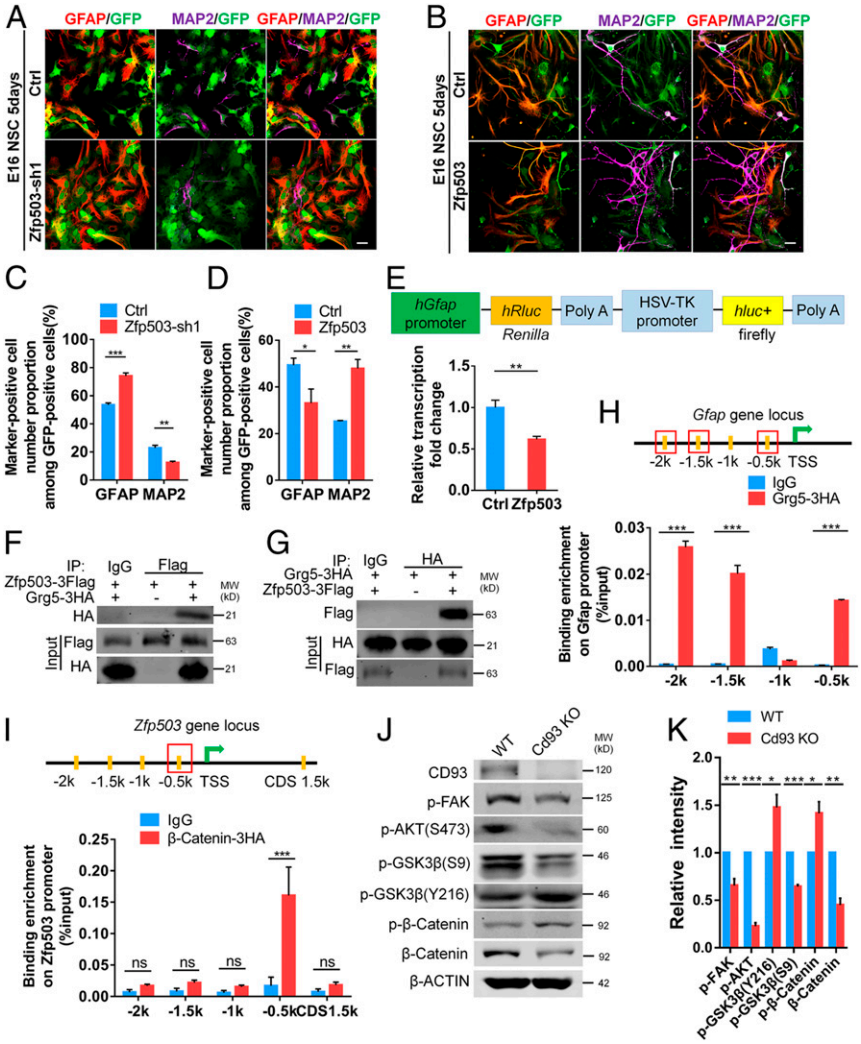

Fig. 7. CD93 regulates astrogenesis through the transcriptional repressor ZFP503. (*A* and *B*) E16 neural stem cells were isolated, infected with the indicated lentivirus, and cultured in differentiation medium for 5 d before being immunostained for GFAP and MAP2. (Scale bars, 20 μm.) (*C* and *D*) The percentage of GFAP- or MAP2-positive cells among all GFP-positive cells in *A* and *B*. $n = 3$ independent experiments. (*E*) A luciferase assay demonstrated that ZFP503 repressed *hGfap* promoter activity. (*Upper*) The *hGfap* promoter was cloned into the psiCheck2 vector. (*Lower*) Quantification of the relative fold change in *Gfap* transcription. $n = 6$ independent experiments. (*F* and *G*) Co-IP experiments tested the interaction between ZFP503 and Grg5 in 293FT cells. (*H*) A Ch-IP assay verified that Grg5 binds to the sites of the *Gfap* promoter. E16 neural stem cells were infected with Grg5-3HA lentivirus and cultured for 4 d before being collected. $n = 3$ independent experiments. (*I*) A Ch-IP assay verified that β-Catenin binds to the site of the *Zfp503* promoter. The assay was performed in N2a cells. $n = 4$ independent experiments. (*J*) The indicated protein levels were detected in the E16 wild-type and *Cd93* knockout cerebral cortex. (*K*) Quantification of the protein levels in *J*. $n = 3$ wild-type mice and 3 *Cd93* knockout mice. Statistical analysis was performed using Student's *t* test for comparisons of two groups and one-way ANOVA for comparisons of more than two groups. The error bars show mean ± SEM; ns, $P > 0.05$; $^{*}P < 0.05$; $^{**}P < 0.01$; $^{***}P < 0.001$.

cascade and that β-Catenin translocates into the nucleus to activate *Zfp503* transcription.

Discussion

Understanding why astrocyte production occurs later than neuron production has attracted the attention of scientists for years. It has gradually become clear that astrogenesis is repressed during the neurogenic period. Over several decades, scientists have explored several different processes, such as DNA methylation, transcriptional repressors, and competitive inhibition by bHLH transcription factors. Here, we identify a critical negative regulator in astrogenesis. Our study focused on CD93, which is the receptor of the ECM protein MMRN2. We demonstrate that CD93 plays a negative role in controlling astrogenesis. CD93 likely functions to maintain the repressed state of astrogenesis after the demethylation of astrocytic gene promoters. As development proceeds, the CD93 level declines, and then astrogenesis occurs gradually. Our study provides evidence of the repression of astrogenesis onset.

CD93 is traditionally considered an immunity-related receptor, and we found that *Cd93* knockout down-regulated a series of genes related to immunity and inflammation (Fig. 6 *B* and *C*). This implies that CD93 participates in the regulation of immunity and inflammation in the brain, and further studies are needed to explore the related functions. Our study showed that *Cd93* knockout increases astrocyte production and that CD93 per se represses the onset of astrogenesis. To validate that the phenotype is due to CD93 loss of function in radial glial cells rather than other influencing factors in conventional knockout mice, we performed experiments to exclude the potential impact of inflammation. CD93 probably plays a neuroprotective role in pathological models when there is inflammation, but *Cd93*

knockout does not cause inflammation. In addition, from the RNA-seq data, we observed that the transcription of a number of ECM proteins that are probably related to the receptor function of CD93 are down-regulated in *Cd93* knockout mice.

In the late embryonic stage, radial glial cells have the ability to differentiate mainly toward astrocytes and partially toward neurons. The increased astrogenesis occurs at the expense of reduced neuron production in *Cd93* knockout mice, and ZFP503 may play roles in neurogenesis in an unknown way. It is likely that other factors downstream of CD93 regulate neurogenesis at this stage. In the RNA-seq data, we observed the down-regulation of a series of transcription factors related to neurogenesis. In our study, we observed increased astrocyte production; however, we did not notice any significant change in the classical pathways that regulate astrogenesis in the RNA-seq data. We hypothesized that there must be an unknown pathway, and we found a pathway and a critical factor, ZFP503, that participate in astrogenesis. In our pathway, β-Catenin is translocated from the cytoplasm to the nucleus, and it functions in differentiation rather than proliferation in the late embryonic stage; this is consistent with a previous study of its role in differentiation in this stage (46).

In conclusion, our study reveals an external and internal signal that regulates the onset of astrogenesis. Our study demonstrated that the CD93 receptor and the transcriptional repressor ZFP503 negatively regulate astrocyte production. Furthermore, there are autism-like behaviors in *Cd93* knockout mice. Together, our study provides insight into a comprehensive understanding of sequential differentiation and the proper timing of astrogenesis onset.

Materials and Methods

A full description of materials and methods is provided in *SI Appendix, Materials and Methods*.

Mice. The ICR pregnant mice for in vitro experiments and C57 pregnant mice for in utero electroporation were purchased from Vital River Laboratories (Beijing, China). The experimental littermates were from the crossing between *Cd93* heterozygous mice. Mice were raised under standard conditions on a 12 h light and 12 h dark cycle. All of the animal experiments involved were performed according to the NIH *Guide for the Care and Use of Laboratory Animals* (47), and all of the animal experimental procedures were approved by the Animal Committee of Institute of Zoology, Chinese Academy of Sciences.

Generation of *Cd93* Knockout Mice. Single-guide RNAs (sgRNAs) were designed and cloned into the pUC57-kan-T7- guide RNA (gRNA) vector. The Cas9-expressing vector used was pST1374-*N*-NLS-FLAG-linker-Cas9. After transcription and purification, the gRNAs and Cas9-expressing vector were microinjected into fertilized single-cell embryos. The Polymerase chain reaction (PCR) experiment was performed to identify the genotype of the offspring. The length of products is about 1,296 bp for wild type and 331 bp for *Cd93* knockout mice. The sgRNAs and genotyping primers are in *SI Appendix*, Table S1.

Immunostaining. Brain-slice samples were fixed in 4% paraformaldehyde and dehydrated in 30% sucrose. Fifteen-micrometer brain slices were obtained using the freezing microtome. Slices or cell samples were fixed in 4% paraformaldehyde for 20 min, washed three times in phosphate-buffered saline (PBS) added with 0.1% Triton X-100, blocked with 5% bovine serum albumin (in PBS) for 1 h, and incubated in primary antibodies at 4 °C overnight. Samples were washed three times and incubated in secondary antibodies for 1 h.

In Utero Electroporation. The pregnant mice (E15) were anesthetized by intraperitoneal injection of sodium pentobarbital. Recombinant plasmid together with Venus-GFP plasmid at a molar ratio of 3:1 (about 2 μL) was gently microinjected into the embryonic lateral ventricle. A total of 1.5 μg/μL pCDH-CMV-MMRN2-EF1-copGFP, pCDH-CMV-MCS-EF1-copGFP, and Venus-GFP was used in the experiment. Five 50-ms pulses with an interval of 950 ms at 45 V were given to brains with an electroporator (BTX ECM830). The mixed plasmids were electroporated into the cells in the ventricular zone. The embryonic brains were harvested 3 d later at E18.

RNA-Sequencing Analysis. Total RNA was extracted from E16 cerebral cortex of wild-type and *Cd93* knockout mice. The following procedures were performed by Annoroad Genomics. After quality control by an Agilent 2100 RNA Nano 6000 Assay Kit, a complementary DNA library was built and used for high-throughput sequencing by Illumina HiSEq. 2500 platform. The genome index was built with Bowtie2 v2.2.3, and clean data were mapped to the reference genome with TopHat v2.0.12. The expression level of genes was estimated by reads per kilobase per million reads (RPKM). The $|\log2 \text{ Fold change}| \geq 1$ and $q < 0.05$ were the statistical criteria for significantly differentially expressed genes. The significant enrichment of gene ontology terms was identified with $q < 0.05$. The data for two pairs of samples were deposited into the Gene Expression Omnibus (GEO) database under accession number GSE134642.

Confocal Imaging and Statistical Analysis. Images for immunostaining were visualized by a Zeiss 780 laser-scanning confocal microscope. In vivo astrocyte and neuron number per image were counted with Photoshop CS6 (Adobe) and divided by the area. Statistical analysis for the area of the cerebral cortex was performed using ImageJ. Statistical analysis was performed using Student's *t* test for comparisons of two groups and one-way or two-way ANOVA for comparisons of more than two groups. Quantitative data were shown as mean ± SEM. The graphs were made by Graphpad prism 6.

Data Availability. The GEO accession number for the transcriptome sequencing data reported in this article is GSE134642.

ACKNOWLEDGMENTS. We thank Wenzheng Zou and Yanxin Li for performing the in utero electroporation; Zhongqiu Li for collecting the blood from the orbit; Yanzhen Xie for plasmid extraction; Shiwen Li and Xili Zhu for confocal imaging; and Hua Qin for behavioral tests. This work was supported by grants from the National Science Fund for Distinguished Young Scholars (81825006); the National Key R&D Program of China (2019YFA0110300); the Chinese Academy of Sciences Strategic Priority Research Program (XDA16020602); the National Science Foundation of China (31730033 and 31621004); and the key deployment projects of the Chinese Academy of Sciences (ZDRW-ZS-2017-5).

1. F. D. Miller, A. S. Gauthier, Timing is everything: Making neurons versus glia in the developing cortex. *Neuron* **54**, 357–369 (2007).
2. X. Qian *et al*., Timing of CNS cell generation a programmed sequence of neuron and glial cell production from isolated murine cortical stem cells. *Neuron* **28**, 69–80 (2000).
3. X. Qian *et al*., Timing of CNS cell generation: A programmed sequence of neuron and glial cell production from isolated murine cortical stem cells. *Neuron* **28**, 69–80 (2000).
4. E. Hartfuss, R. Galli, N. Heins, M. Götz, Characterization of CNS precursor subtypes and radial glia. *Dev. Biol.* **229**, 15–30 (2001).
5. S. M. Culican, N. L. Baumrind, M. Yamamoto, A. L. Pearlman, Cortical radial glia: Identification in tissue culture and evidence for their transformation to astrocytes. *J. Neurosci.* **10**, 684–692 (1990).
6. A. R. Kriegstein, M. Götz, Radial glia diversity: A matter of cell fate. *Glia* **43**, 37–43 (2003).
7. T. E. Anthony, C. Klein, G. Fishell, N. Heintz, Radial glia serve as neuronal progenitors in all regions of the central nervous system. *Neuron* **41**, 881–890 (2004).
8. J. G. Parnavelas, B. Nadarajah, Radial glial cells: Are they really glia? *Neuron* **31**, 881–884 (2001).
9. T. Takizawa *et al*., DNA methylation is a critical cell-intrinsic determinant of astrocyte differentiation in the fetal brain. *Dev. Cell* **1**, 749–758 (2001).
10. G. Fan *et al*., DNA methylation controls the timing of astrogliogenesis through regulation of JAK-STAT signaling. *Development* **132**, 3345–3356 (2005).
11. Y. Sun *et al*., Neurogenin promotes neurogenesis and inhibits glial differentiation by independent mechanisms. *Cell* **104**, 365–376 (2001).
12. O. Hermanson, K. Jepsen, M. G. Rosenfeld, N-CoR controls differentiation of neural stem cells into astrocytes. *Nature* **419**, 934–939 (2002).
13. K. Nakashima *et al*., BMP2-mediated alteration in the developmental pathway of fetal mouse brain cells from neurogenesis to astrocytogenesis. *Proc. Natl. Acad. Sci. U.S.A.* **98**, 5868–5873 (2001).
14. A. Bonni *et al*., Regulation of gliogenesis in the central nervous system by the JAK-STAT signaling pathway. *Science* **278**, 477–483 (1997).
15. M. A. Bonaguidi *et al*., LIF and BMP signaling generate separate and discrete types of GFAP-expressing cells. *Development* **132**, 5503–5514 (2005).
16. M. K. Taylor, K. Yeager, S. J. Morrison, Physiological Notch signaling promotes gliogenesis in the developing peripheral and central nervous systems. *Development* **134**, 2435–2447 (2007).
17. C. S. Barros, S. J. Franco, U. Müller, Extracellular matrix: Functions in the nervous system. *Cold Spring Harb. Perspect. Biol.* **3**, a005108 (2011).
18. Y. C. Li, Y. C. Lin, T. H. Young, Combination of media, biomaterials and extracellular matrix proteins to enhance the differentiation of neural stem/precursor cells into neurons. *Acta Biomater.* **8**, 3035–3048 (2012).

19. J. C. Xu *et al*., The extracellular matrix glycoprotein tenascin-R regulates neurogenesis during development and in the adult dentate gyrus of mice. *J. Cell Sci.* **127**, 641–652 (2014).
20. S. Raghavan, R. R. Gilmont, K. N. Bitar, Neuroglial differentiation of adult enteric neuronal progenitor cells as a function of extracellular matrix composition. *Biomaterials* **34**, 6649–6658 (2013).
21. A. Faissner, J. Reinhard, The extracellular matrix compartment of neural stem and glial progenitor cells. *Glia* **63**, 1330–1349 (2015).
22. L. S. Campos, L. Decker, V. Taylor, W. Skarnes, Notch, epidermal growth factor receptor, and beta1-integrin pathways are coordinated in neural stem cells. *J. Biol. Chem.* **281**, 5300–5309 (2006).
23. M. F. Brizzi, G. Tarone, P. Defilippi, Extracellular matrix, integrins, and growth factors as tailors of the stem cell niche. *Curr. Opin. Cell Biol.* **24**, 645–651 (2012).
24. O. Petrenko *et al*., The molecular characterization of the fetal stem cell marker AA4. *Immunity* **10**, 691–700 (1999).
25. M. C. Greenlee-Wacker, M. D. Galvan, S. S. Bohlson, CD93: Recent advances and implications in disease. *Curr. Drug Targets* **13**, 411–420 (2012).
26. M. C. Greenlee, S. A. Sullivan, S. S. Bohlson, CD93 and related family members: Their role in innate immunity. *Curr. Drug Targets* **9**, 130–138 (2008).
27. E. P. McGreal, N. Ikewaki, H. Akatsu, B. P. Morgan, P. Gasque, Human C1qRp is identical with CD93 and the mNI-11 antigen but does not bind C1q. *J. Immunol.* **168**, 5222–5232 (2002).
28. D. Harhausen *et al*., CD93/AA4.1: A novel regulator of inflammation in murine focal cerebral ischemia. *J. Immunol.* **184**, 6407–6417 (2010).
29. M. R. Griffiths, M. Botto, B. P. Morgan, J. W. Neal, P. Gasque, CD93 regulates central nervous system inflammation in two mouse models of autoimmune encephalomyelitis. *Immunology* **155**, 346–355 (2018).
30. R. R. Nepomuceno, A. H. Henschen-Edman, W. H. Burgess, A. J. Tenner, cDNA cloning and primary structure analysis of C1qR(P), the human C1q/MBL/SPA receptor that mediates enhanced phagocytosis in vitro. *Immunity* **6**, 119–129 (1997).
31. P. J. Norsworthy *et al*., Murine CD93 (C1qRp) contributes to the removal of apoptotic cells in vivo but is not required for C1q-mediated enhancement of phagocytosis. *J. Immunol.* **172**, 3406–3414 (2004).
32. F. Galvagni *et al*., Dissecting the CD93-Multimerin 2 interaction involved in cell adhesion and migration of the activated endothelium. *Matrix Biol. J. Int. Soc. Matrix Biol.* **64**, 112–127 (2017).
33. K. A. Khan *et al*., Multimerin-2 is a ligand for group 14 family C-type lectins CLEC14A, CD93 and CD248 spanning the endothelial pericyte interface. *Oncogene* **36**, 6097–6108 (2017).
34. R. Lugano *et al*., CD93 promotes β1 integrin activation and fibronectin fibrillogenesis during tumor angiogenesis. *J. Clin. Invest.* **128**, 3280–3297 (2018).
35. S. J. Ji, G. Periz, S. Sockanathan, Nolz1 is induced by retinoid signals and controls motoneuron subtype identity through distinct repressor activities. *Development* **136**, 231–240 (2009).
36. M. Nakamura, A. P. Runko, C. G. Sagerström, A novel subfamily of zinc finger genes involved in embryonic development. *J. Cell. Biochem.* **93**, 887–895 (2004).
37. A. P. Runko, C. G. Sagerström, Isolation of nlz2 and characterization of essential domains in Nlz family proteins. *J. Biol. Chem.* **279**, 11917–11925 (2004).
38. P. Shahi *et al*., The transcriptional repressor ZNF503/Zeppo2 promotes mammary epithelial cell proliferation and enhances cell invasion. *J. Biol. Chem.* **290**, 3803–3813 (2015).
39. A. Kumar *et al*., Zfp703 is a Wnt/β-catenin feedback suppressor targeting the β-Catenin/Tcf1 complex. *Mol. Cell. Biol.* **36**, 1793–1802 (2016).
40. E. M. Slorach, J. Chou, Z. Werb, Zeppo1 is a novel metastasis promoter that represses E-cadherin expression and regulates p120-catenin isoform expression and localization. *Genes Dev.* **25**, 471–484 (2011).
41. S. K. Mitra, D. A. Hanson, D. D. Schlaepfer, Focal adhesion kinase: In command and control of cell motility. *Nat. Rev. Mol. Cell Biol.* **6**, 56–68 (2005).
42. P. E. Hall, J. D. Lathia, N. G. Miller, M. A. Caldwell, C. ffrench-Constant, Integrins are markers of human neural stem cells. *Stem Cells* **24**, 2078–2084 (2006).
43. M. S. Samuel *et al*., Actomyosin-mediated cellular tension drives increased tissue stiffness and β-catenin activation to induce epidermal hyperplasia and tumor growth. *Cancer Cell* **19**, 776–791 (2011).
44. J. K. Mouw *et al*., Tissue mechanics modulate microRNA-dependent PTEN expression to regulate malignant progression. *Nat. Med.* **20**, 360–367 (2014).
45. C. M. Warboys, Mechanoactivation of Wnt/β-catenin pathways in health and disease. *Emerg. Top. Life Sci.* **2**, 701–712 (2018).
46. R. N. Munji, Y. Choe, G. Li, J. A. Siegenthaler, S. J. Pleasure, Wnt signaling regulates neuronal differentiation of cortical intermediate progenitors. *J. Neurosci.* **31**, 1676–1687 (2011).
47. National Research Council, *Guide for the Care and Use of Laboratory Animals* (National Academies Press, Washington, DC, ed. 8, 2011).